MULTI-SENSOR ASSESSMENT OF TRENDS IN ATTRIBUTES OF VEGETATION DYNAMICS AND ECOSYSTEM FUNCTIONING DERIVED FROM NDVI TIME SERIES

Bruno Marcos[1], Isabel Pôças[1], João Gonçalves[1] and João Pradinho Honrado[1,2]

1. CIBIO-Centro de Investigação em Biodiversidade e Recursos Genéticos, Universidade do Porto Campus Agrário de Vairão, Rua Padre Armando Quintas, Crasto. 4485-661 Vairão, Portugal; bruno.marcos@fc.up.pt
2. Departamento de Biologia, Faculdade de Ciências da Universidade do Porto, Edifício FC4, Rua do Campo Alegre, S/N. 4169-007 Porto, Portugal.

ABSTRACT

Vegetation Indices derived from Earth Observation Satellite data have been broadly used for a wide range of ecological applications. One of such applications is vegetation monitoring. Properties of NDVI time series can be summarized in several metrics of the NDVI annual curve, including metrics that measure attributes related with primary production and with phenology, which can provide information about the condition and functioning of vegetation and ecosystems, related with the exchanges of matter and energy. In this study, we use a consistency analysis approach to compare the inter-annual trends in attributes of vegetation dynamics and ecosystem functioning obtained from two NDVI time series products, from two different satellite sensors (Terra/MODIS and SPOT/VGT2). We also discuss the use of outputs from analyses based on data from multiple sensors to enhance the assessment and monitoring of condition and changes in such attributes. Results show low consistency in trends of the selected metrics, between the two datasets used, including the relative proportions of significant and non-significant, and positive and negative trends detected, as well as in the magnitude of the trends detected. Thus, the use of different datasets and/or sensors for the assessment of trends in attributes of vegetation dynamics and ecosystem functioning can potentially lead to different conclusions about environmental condition and change at regional scale, which can have an impact on reporting, management policies, and decision-making. To cope with this problem, when evaluation of the accurateness of the results (i.e. validation with ground truth like, e.g., phenological observations with dedicated stations) is not available and/or possible, we suggest using a consistency analysis of outputs from two (or more) different sources (i.e. datasets/sensors), like the one employed in this study. This approach allows to identify the main areas where the main trends in attributes of vegetation dynamics and ecosystem functioning are likely to have occurred, within a target region and period of time.

INTRODUCTION

Worldwide concerns about the impact of global change on the structural and functional response of ecosystems give rise to the need of implementing efficient monitoring tools aiming for tracking and understanding environmental and ecological change.

Vegetation Indices (VIs) derived from Earth observation satellite data have been broadly used for a wide range of environmental and ecological applications (1). One of such applications is vegetation monitoring, due to the scalable relations of this type of data with several plant biophysical parameters, e.g. (2,3,4,5). Particularly, the Normalized Difference Vegetation Index (NDVI) is strongly related to the fraction of the incoming photosynthetically active radiation (fPAR) intercepted by green vegetation, and it has been widely used for monitoring changes in ecosystem structure and function (6,7,8), monitoring biodiversity state and change through species detection or modelling (9,10,11), detecting long-term trends in vegetation growth and phenology (12,13,14), providing inputs for primary production (15) , and a reference to model carbon balance worldwide (16).

Properties of NDVI time series can be summarized in several attributes of the NDVI annual curve, including attributes related with primary production (e.g. (17)) and with phenology (e.g. (18)), which can provide information about the condition and functioning of vegetation and ecosystems (e.g. (8,19,20,21,22,23)). Such functional attributes are related with the exchanges of matter and energy and have a shorter response time to environmental changes (when compared to structural attributes), thus allowing a better understanding of large-scale ecological changes associated to ecosystem function and processes (19,24,25).

In this sense, NDVI time series datasets, like the ones derived from the Moderate Resolution Imaging Spectroradiometer (MODIS) and the Satellite Pour L'Observation de la Terre – VEGETATION (SPOT-VGT) sensors, hold considerable promise for spatially continuous characterization and monitoring of changes in vegetation dynamics and ecosystem functioning at regional scales (e.g. (19,23)), given their global coverage, intermediate spatial resolution (250m to 1km), high temporal resolution (data aggregated in 10- to 16-day composites), availability (since 2000 and 1998, respectively), and free-of-charge status (6).

Temporal analysis of data from satellite sensors with high temporal resolution has become increasingly popular (e.g. (26,27,28,29), with particular attention being given to the detection and measurement of intra- and /or inter-annual trends in NDVI values (12,14,28,30,31,32,33). However, there are relatively few studies comparing different datasets ((e.g. (30)), and even less from different sensors (e.g. (14)), for those purposes. Furthermore, trend analysis is often used to evaluate changes in NDVI values, but seldom used to evaluate changes in ecosystem functional attributes extracted from those values (e.g. (26)).

In this work, we aimed to assess if there are significant differences between inter-annual trends of key ecosystem functional attributes obtained from two different sensors, in this case MODIS and VGT. To do so, we evaluated inter-annual trends in several attributes of the NDVI curves using time series datasets from both sensors, for the period 2003–2010, in the northern half of mainland Portugal. We also point some directions regarding the use of outputs from analyses based on data from multiple sensors to enhance the assessment of trends in such attributes. Finally, we discuss implications of our results for the assessment and monitoring of ecosystem state and trends as well as for the timely and robust detection of ecological change.

TEST AREA AND MATERIAL

Test area

The test area comprises the northern part of continental Portugal, which includes the westernmost transition between the Atlantic and Mediterranean environmental zones of Europe (34)). This area is characterized by a wide heterogeneity in elevation, ranging from 0 to 1993 metres, thus resulting in a great variation of environmental conditions, namely climate and soils. Native forests are dominated by deciduous broadleaved trees in Atlantic areas and by evergreen sclerophyllous trees in Mediterranean areas. Evergreen forest plantations of eucalypts and pines, together with a high diversity of agricultural land use types and urban areas, further contribute to enhance landscape heterogeneity. Furthermore, this area is located within the Iberian Peninsula, which is considered to be a very dynamic area in relation to global change and ecosystem functioning (19).

Satellite datasets

The 16-day Terra MODIS NDVI product at 1 km spatial resolution (MOD13A2, Collection 5) is based on the Terra MODIS level 2 (L2G) daily surface reflectance product (MOD09 series), which provides red and near-infrared surface reflectance corrected for the effect of atmospheric gases, thin cirrus clouds and aerosols. This product includes a data quality assessment layer (QA binary data) and a pixel reliability layer holding information on overall usefulness and cloud conditions on a per-pixel basis (35).

The SPOT-VEGETATION 10-day composite NDVI synthesis product (S10) provides a Maximum Value Composite (MVC; (36)) at full spatial resolution (1 km). This product includes corrections for

molecular and aerosol scattering, water vapour, ozone and other gas absorption, and for misregistration of the different channels, as well as calibration of all the detectors along the line-array detectors for each spectral band. Status maps are provided for each S10 product including per-pixel cloud-cover information (37).

Although data is available from February 2000 and April 1998, for MODIS MOD13A2 and SPOT-VEGETATION S10 products respectively, in this study we used only the composites from January 2003 to December 2010, from both datasets, because of the SPOT-VEGETATION sensor swap from the one on board the SPOT-4 satellite (VGT1) to the one on board the SPOT-5 satellite (VGT2).(14) reported a significant shift in NDVI values after this change, and explained it by differences in the design of the VGT1 and VGT2 red and near-infrared spectral bands.

Table 1 presents a summary of the main characteristics of both.

In order to make the MODIS and VGT datasets more directly comparable, we: (i) projected all the data to the WGS84 / UTM zone 29 N reference system; and (ii) converted the VGT status maps to a quality flags scheme compatible with MODIS' Pixel Reliability layers.

Table 1: Main characteristics of the datasets/sensors used in this study.

	MODIS	*VGT*
Satellite/sensor	Terra/MODIS	SPOT-5/VGT2
Availability	Since February 2000	Since January 2003
Equator-crossing time	10.30 am	10.30 am
Product	MOD13A2	S10
Spatial resolution	1 km	1 km
Spatial reference system	Sinusoidal projection	Plate-Carrée geographic projection
Temporal frequency	16-days MVC	10-day MVC
Number of images per year	23	36
Radiometric resolution	12-bit (4096 levels)	8-bit (256 levels)
Red band wavelength interval	620-670 nm	615-690 nm
NIR band wavelength interval	841-876 nm	782-890 nm

Preprocessing

Remotely sensed, per-pixel time series of the Normalized Difference Vegetation Index (NDVI) can be hindered by noise from different sources (e.g. presence of clouds, varying sun-sensor-viewing geometries; (38)). To address this issue, we used a blind rejection approach (i.e. without prior knowledge of the quality of the data) for data cleaning and smoothing, in order to remove spurious values.

Firstly, we employed a filter based on the Hampel identifier (39), which uses the concept of breakdown points based on local estimations of the median absolute deviation (MAD) and replaces the identified outliers with a local median. The Hampel identifier is often considered extremely effective (40).

Secondly, we used a Savitzky-Golay filter, in order to further remove and replace spurious values. Savitzky-Golay filters (41) have been increasingly applied for cleaning, smoothing, and reconstruction of NDVI time series (42,43).

All computations mentioned in this section were performed using the R programming environment (44).

ANALYTICAL FRAMEWORK

Extraction of ecosystem functional attributes

The extraction of ecosystem functional attributes from temporal profiles of remote sensing-derived variables (e.g. vegetation indices like NDVI) has gained considerable attention in the last years. To this end, numerous methods, based on a wide range of techniques, have been used. One of the most broadly used software packages for such purposes is TIMESAT (18,45,46,47,48), which implements different methods to fit the upper envelope of NDVI data and allows the use of quality flags (i.e. pixel reliability) to assign weights as measures of the uncertainty in the NDVI data.

In this work, we used TIMESAT's Double Logistic function-fitting method to extract metrics of the NDVI annual curves that are related to key attributes of vegetation dynamics and ecosystem functioning. Double Logistic has been used for some time (22,49) and is currently one of the best performing techniques available to fit NDVI annual curves (50).

We selected six of the eleven metrics directly computed by TIMESAT, based on their ecological relevance ((25); Table 2). Three of them are measures of variability in productivity (i.e. seasonality of vegetation growth) and overall productivity during the growing season ("Seasonal amplitude", "Largest data value for the fitted function", and "Large seasonal integral"), and the other three are indicators of phenology (i.e. timing of key parameters of the growing season: "Time for the start of the season", "Time for the mid of the season", and "Time for the end of the season"). We then compared the major patterns of the yearly median values for each pixel and metric, between datasets, by visual inspection of corresponding maps and density plots.

Table 2: TIMESAT metrics used in this study, with corresponding key attributes of vegetation dynamics and ecosystem functioning. For more information on the metrics available in TIMESAT, see (46,47).

TIMESAT designation	*Short name*	*Ecological meaning*
Seasonal amplitude	AMP	Intra-annual variability (i.e. seasonality) of primary production
Largest data value for the fitted function during the season	FMX	Maximum level of photosynthetic activity/primary production
Large seasonal integral	LSI	Cumulative primary production during the growing season
Time for the start of the season	SOS	Date of the start of the vegetation growing (green-up)
Time for the mid of the season	MOS	Proxy of the date of maximum photosynthetic activity
Time for the end of the season	EOS	Date of the end of the vegetation growing (senescence)

Evaluation of temporal trend patterns and consistency

In order to evaluate the direction and magnitude of inter-annual trends for each of the metrics analyzed, we used the Theil–Sen's non-parametric statistical test. The Theil–Sen's test is a rank-based test which is robust against non-normality of the distribution and missing values (51), and unlike the Mann–Kendall test, it detects not only if a trend exists, but also provides the amplitude of that trend (52). For this purpose, we used the R package zyp (53), which accounts for inter-annual autocorrelation present in the data.

To assess the level of consistency between the trends obtained from the different datasets, we applied a classification scheme adapted from (30) in order to get a single outcome for each pixel

(representing the level of consistency), from the combination of the trend slope and p-value obtained from each datasets. For that purpose, the trend slopes and p-values from each dataset were classified into statistically significant ("Negative" or "Positive") and non-significant trends ("Absence"), assuming significant slopes for p-values < 0.1. Consensus maps were then produced from the results of this classification process. Table 3 illustrates the classification scheme employed.

Table 3: Classification scheme combining the temporal trends from both datasets/sensors used (MODIS and VGT).

	Negative (VGT)	*Absence (VGT)*	*Positive (VGT)*
Negative (MODIS)	Consistent negative	Likely negative	Uncertain/ambiguous
Absence (MODIS)	Likely negative	Consistent absence	Likely positive
Positive (MODIS)	Uncertain/ambiguous	Likely positive	Consistent positive

Comparison of trend magnitudes between datasets, for each metric, was carried out by visual inspection of the corresponding density plots and consensus maps. We used chi-squared tests in order to evaluate differences in the proportions of each trend class ("Negative", "Positive" or "Absence") between datasets. Finally, we looked for major spatial clusters of identified statistically significant trends, by applying simple majority filters (i.e. choosing, for each pixel, the most frequent trend class in the corresponding 3×3 pixels spatial vicinity) to the consensus maps.

RESULTS AND DISCUSSION

Regional patterns of ecosystem functional attributes

The spatial distributions of the selected TIMESAT metrics obtained from the two datasets used in this study (i.e. MODIS and VGT) reveal similar overall geographic patterns of key attributes of vegetation dynamics and ecosystem functioning in the test area (Figure 1).

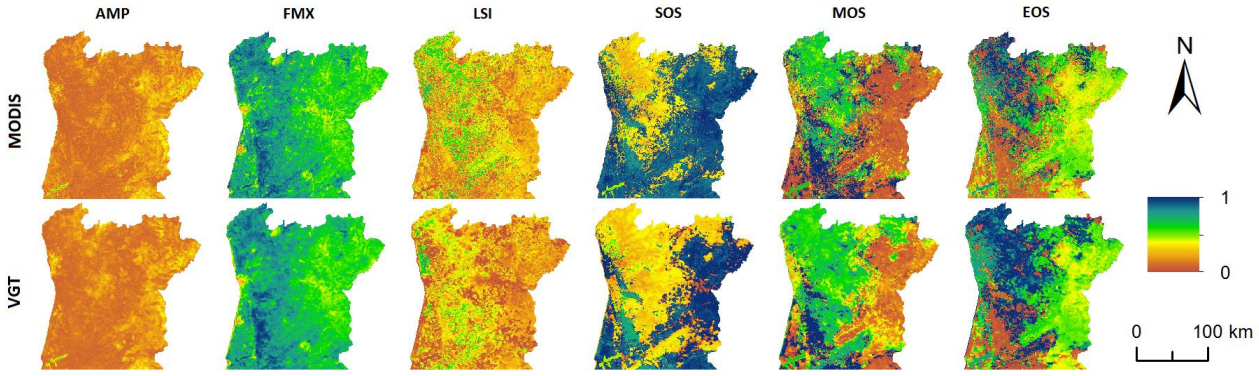

Figure 1: Maps of the yearly median results for the selected TIMESAT metrics for the test area – "Seasonal amplitude" (AMP), "Largest data value for the fitted function during the season" (FMX), "Large seasonal integral" (LSI), "Time for the start of the season" (SOS), "Time for the mid of the

season" (MOS), and "Time for the end of the season" (EOS). Metrics AMP, FMX and LSI are dimensionless. Values of metrics SOS, MOS and EOS can be read as "relative time of the year", with "0" corresponding to the beginning of the year (i.e. January 1st) and "1" corresponding to the end of the year (i.e. December 31st). Maps on the top row show results of metrics obtained using the MODIS dataset, whereas the maps on the bottom row show the ones obtained using the VGT dataset.

Visual comparison of the yearly median of each metric's density plots (Figure 2) show that the general shape of the curves are similar between datasets, with fewer differences in the distribution of values for the metrics related to primary production (Figure 2a,b,c) than those for the phenology metrics (Figure 2d,e,f). The former tend to follow approximately uni-modal distributions of values, with the respective central tendency (in this case, the median) for both datasets being very close to each other, whereas the latter tend to exhibit multi-modal distributions of values, with two or more main peaks that are generally located around the same values, but with differences in the relative densities of each peak between datasets.

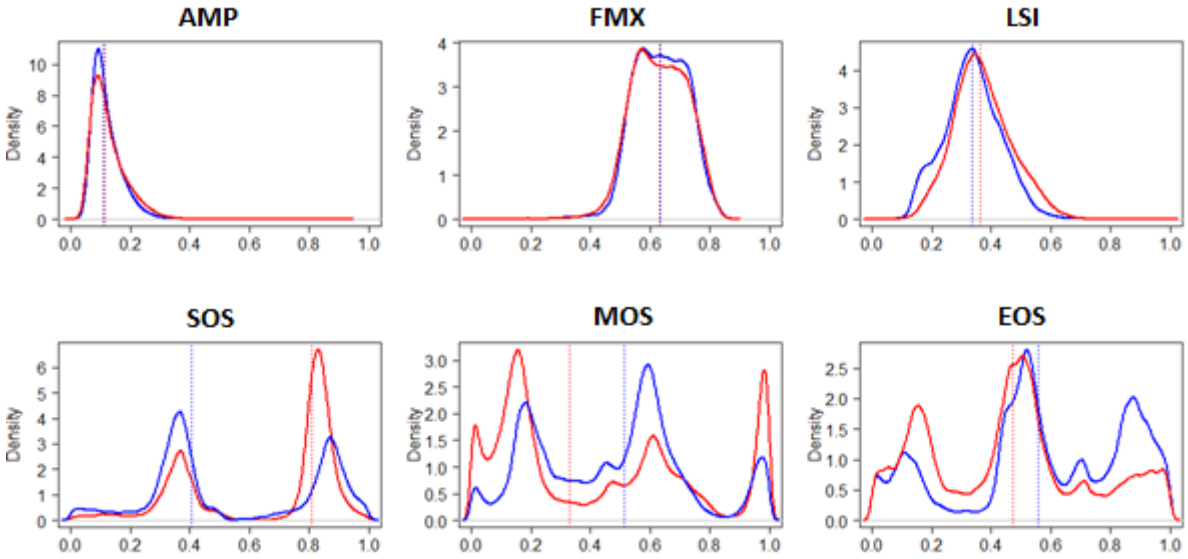

Figure 2: Distributions of values of the yearly median for each metric calculated from the two datasets used: MODIS (red bold lines) and VGT (blue bold lines) – "Seasonal amplitude" (AMP), "Largest data value for the fitted function during the season" (FMX), "Large seasonal integral" (LSI), "Time for the start of the season" (SOS), "Time for the mid of the season" (MOS), and "Time for the end of the season" (EOS). Dotted lines correspond to the respective median values (MODIS in red and VGT in blue), as an indication of central tendency.

The observed patterns suggest that attributes of vegetation dynamics and ecosystem functioning more related with primary production have a more gradual variation within the test area, while the phenological attributes exhibit more evident geographic transitions, which can be related with the main regional patterns of vegetation types driven by climatic and land use heterogeneity. Moreover, the stronger differences in the phenology-related metrics can also result from the differences in the temporal resolution of the data used: 10-day composites from SPOT-VGT vs. 16-day composites from MODIS.

Regional patterns and consistency of temporal trends

Analysis of trend slope values through using density plots reveal large discrepancies between trends for the selected metrics between the two datasets (Figure 3). When only the statistically significant slopes are considered, the values tend to exhibit a bi-modal distribution, with one peak in the negative trend region and the other in the positive trend region.

Trend analysis consistently identified more statistically significant positive trends from MODIS data than from VGT data, across the TIMESAT metrics considered, except for FMX. Conversely, a larger number of significant negative trends were identified in the test area from VGT data than from MODIS data (Figure 3). Comparison of proportions of pixels with significant (Negative or Positive) and non-significant (Absence) trends with chi-squared tests confirmed these results, since differences in the proportions of each trend type were found statistically significant (p-values << 0.1, for all cases, thus rejecting the null hypothesis of equal proportions).

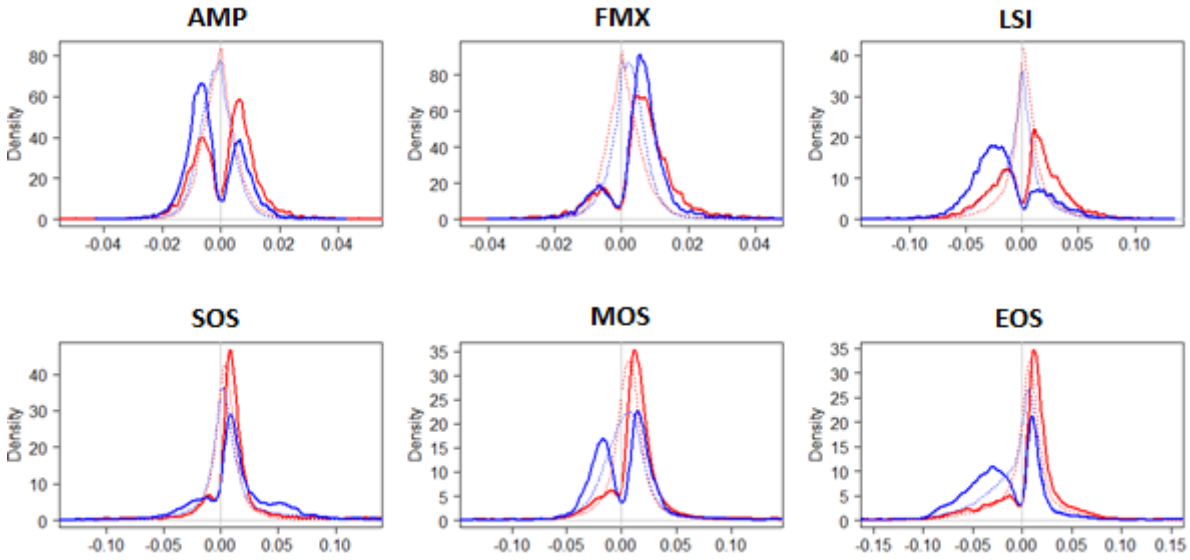

Figure 3: Distributions of slope values of each metric calculated from the two datasets used: MODIS (red) and VGT (blue) – "Seasonal amplitude" (AMP), "Largest data value for the fitted function during the season" (FMX), "Large seasonal integral" (LSI), "Time for the start of the season" (SOS), "Time for the mid of the season" (MOS), and "Time for the end of the season" (EOS). Bold lines correspond to the density of slope values with significant trends (p < 0.1), whereas dotted lines correspond to the density of all slope values, for reference purposes.

In terms of trend magnitudes (positive and negative), the slope values obtained for the AMP and FMX metrics are centred around 0.007–0.008 year^{-1}, and around 0.020–0.028 year^{-1} for the LSI metric (Table 5). For the phenology metrics, the median values of the slopes obtained are 0.011–0.023 year·year^{-1} for the SOS metrics, 0.016–0.020 year·year^{-1} for the MOS metrics, and 0.012–0.039 year·year^{-1} for the EOS metric. Table 5 summarizes the values of the trend slopes for the metrics analysed.

Table 5: Summary of the main characteristics of the trend slope values: minimum (Min.) and maximum (Max.) absolute value, quantile 25% (Q1) and quantile 75% (Q3), and median of the negative (Median (-)) and positive (Median (+)) values. Units for metrics AMP, FMX and LSI are year^{-1}, whereas units for metrics SOS, MOS and EOS are year·year^{-1}.

	Negative	*Positive*

		Min.	Q1	Median(-)	Median (+)	Q3	Max.
AMP	MODIS	-0.110	-0.011	-0.007	0.007	0.011	0.132
	VGT	-0.041	-0.010	-0.008	0.007	0.010	0.041
FMX	MODIS	-0.065	-0.012	-0.008	0.008	0.069	0.069
	VGT	-0.039	-0.011	-0.007	0.008	0.068	0.068
LSI	MODIS	-0.150	-0.034	-0.021	0.020	0.033	0.130
	VGT	-0.152	-0.040	-0.028	0.022	0.035	0.131
SOS	MODIS	-0.167	-0.033	-0.015	0.011	0.018	0.196
	VGT	-0.239	-0.038	-0.023	0.015	0.037	0.275
MOS	MODIS	-0.244	-0.031	-0.018	0.016	0.024	0.212
	VGT	-0.299	-0.029	-0.020	0.018	0.028	0.243
EOS	MODIS	-0.324	-0.054	-0.039	0.016	0.026	0.258
	VGT	-0.367	-0.057	-0.038	0.012	0.020	0.329

We found that per-pixel full consistency between significant trends obtained from the two datasets used was low, for all TIMESAT metrics considered. Consistent negative pixels accounted for less than 1% (from 0.1% for SOS to 0.8% for AMP) of the test area, with Likely negative outcomes (pixels where a significant negative trend was found for only one of the two datasets – a partial consistency) between 1.9% and 10.8% of the total number of pixels. Pixels with Consistent positive trends ranged between 0.4% (LSI) and 2.3% (FMX) of the test area, with Likely positive pixels (i.e. a partial consistency, where significant positive trends were found for only one of the two datasets) accounting for 2.2% to 10.8% of the test area. Inconsistent (i.e. Uncertain/ambiguous) trends between sensors were found for 0.1% (MOS) to 1.1% of the pixels (see Table 6).

Table 6: Contingency tables showing the consensus between datasets in the percentage of pixels that exhibited significant trends ("Negative" or "Positive") or non-significant trends ("Absence") (p-value < 0.1).

a) AMP

	Negative (VGT)	*Absence (VGT)*	*Positive (VGT)*	***Total (VGT)***
Negative (MODIS)	276 (0.8%)	1374 (4.0%)	48 (0.1%)	**1,698 (4.9%)**
Absence (MODIS)	2,647 (7.6%)	26,561 (76.5%)	1,338 (3.9%)	**30,546 (87.9%)**
Positive (MODIS)	204 (0.6%)	2,007 (5.8%)	283 (0.8%)	**2,494 (7.2%)**
Total (MODIS)	**3,127 (9.0%)**	**29,942 (86.2%)**	**1,669 (4.8%)**	**34,738 (100.0%)**

b) FMX

	Negative (VGT)	*Absence (VGT)*	*Positive (VGT)*	***Total (VGT)***
Negative (MODIS)	93 (0.3%)	677 (2.0%)	82 (0.2%)	**852 (2.5%)**
Absence (MODIS)	849 (2.4%)	25,909 (74.6%)	3,427 (9.9%)	**30,185 (86.9%)**
Positive (MODIS)	69 (0.2%)	2,836 (8.2%)	804 (2.3%)	**3,709 (10.7%)**
Total (MODIS)	**1,011 (2.9%)**	**29,422 (84.7%)**	**4,313 (12.4%)**	**34,746 (100.0%)**

c) LSI

	Negative (VGT)	*Absence (VGT)*	*Positive (VGT)*	***Total (VGT)***
Negative (MODIS)	270 (0.8%)	1,497 (4.3%)	65 (0.2%)	**1,832 (5.3%)**

Absence (MODIS)	3,180 (9.2%)	25,914 (74.6%)	1,083 (3.1%)	**30,177 (86.88%)**
Positive (MODIS)	320 (0.9%)	2,254 (6.5%)	151 (0.4%)	**2,725 (7.9%)**
Total (MODIS)	**3,770 (10.9%)**	**29,665 (85.4%)**	**1,299 (3.7%)**	**34,746 (100.0%)**

d) SOS

	Negative (VGT)	*Absence (VGT)*	*Positive (VGT)*	***Total (VGT)***
Negative (MODIS)	28 (0.1%)	656 (1.9%)	32 (0.1%)	**716 (2.1%)**
Absence (MODIS)	679 (2.0%)	28,248 (81.3%)	1,895 (5.5%)	**30,822 (88.7%)**
Positive (MODIS)	48 (0.1%)	2,808 (8.1%)	354 (1.0%)	**3,210 (9.2%)**
Total (MODIS)	**755 (2.17%)**	**31,712 (91.3%)**	**2,281 (6.6%)**	**34,748 (100.0%)**

e) MOS

	Negative (VGT)	*Absence (VGT)*	*Positive (VGT)*	***Total (VGT)***
Negative (MODIS)	124 (0.4%)	823 (2.4%)	27 (0.1%)	**974 (2.8%)**
Absence (MODIS)	2,221 (6.4%)	25,273 (72.7%)	2,401 (6.9%)	**29,895 (86.0%)**
Positive (MODIS)	178 (0.5%)	3,118 (9.0%)	583 (1.7%)	**3,879 (11.2%)**
Total (MODIS)	**2,523 (7.3%)**	**29,214 (84.1%)**	**3,011 (8.7%)**	**34,748 (100.0%)**

f) EOS

	Negative (VGT)	*Absence (VGT)*	*Positive (VGT)*	***Total (VGT)***
Negative (MODIS)	259 (0.8%)	1,211 (3.45%)	68 (0.2%)	**1,538 (4.4%)**
Absence (MODIS)	3,745 (10.8%)	22,474 (64.7%)	2,084 (6.0%)	**28,303 (81.5%)**
Positive (MODIS)	377 (1.1%)	3,762 (10.8%)	768 (2.2%)	**4,907 (14.1%)**
Total (MODIS)	**4,381 (12.6%)**	**27,447 (79.0%)**	**2,920 (8.4%)**	**34,748 (100.0%)**

In the consensus maps for the six metrics considered (Figure 4), some patterns related with the main vegetation types could be recognized in terms of spatial distribution of trend classes. For example, areas dominated by Mediterranean vegetation types (the eastern part of the test area) showed lower density of pixels with statistically significant trends for the metrics of primary production (i.e. AMP, FMX and LSI) than areas typically with Atlantic vegetation types (in the western part of the test area). These differences may be explained by factors such as land cover change or variations in dominant species composition and relative abundance. Concerning the phenology metrics (i.e. SOS, MOS and EOS), the Mediterranean areas showed predominantly positive trends, suggesting that a general tendency for a delay in the vegetation growing season in the considered period (2003–2010) might have occurred. Atlantic areas show predominantly negative trends, which conversely suggest a general tendency for the vegetation growing season to occur earlier in the year. Full consistency, i.e. consistent significant trends (negative or positive), was, as mentioned above, not frequently found, being the majority of significant trends classified as Likely negative or Likely positive, meaning that a statistically significant trend was found only for one of the two datasets (i.e. partial consistency). Nonetheless, pixels with full consistency of trends were often found surrounded by pixels with partial consistent trends, whereas pixels with inconsistent (i.e. classified as Uncertain/ambiguous) were also seldom found, but with a scattered spatial distribution.

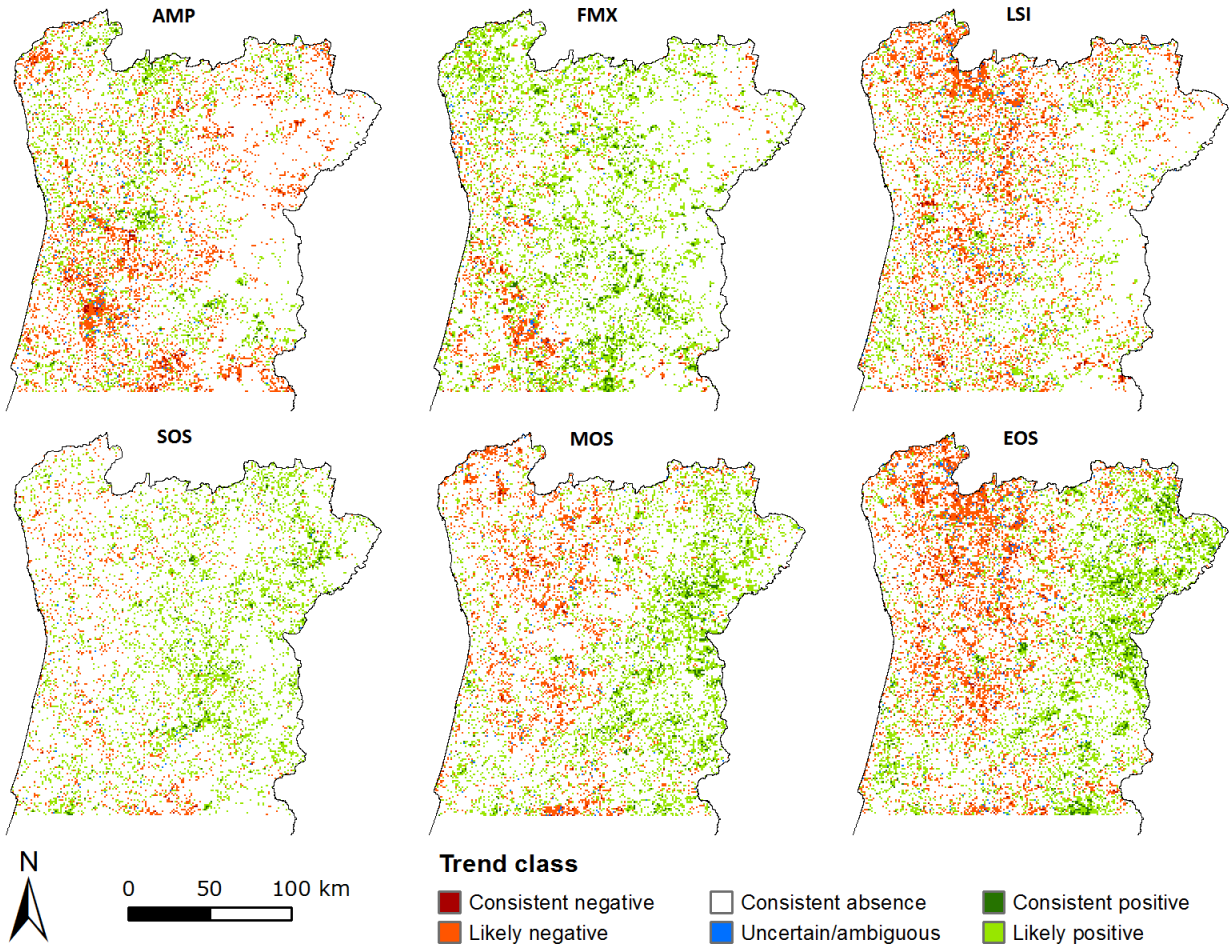

Figure 4: Consensus maps for the analysis of trends in selected TIMESAT metrics) – "Seasonal amplitude" (AMP), "Largest data value for the fitted function during the season" (FMX), "Large seasonal integral" (LSI), "Time for the start of the season" (SOS), "Time for the mid of the season" (MOS), and "Time for the end of the season" (EOS). Classification of trends was based on the combinations of the types of trends ("Negative", "Positive" or "Absence") from each dataset used (MODIS and VGT; see Table 3).

Spatial generalization of consensus maps (Figure 5), aimed at identifying the main spatial clusters (i.e. spatially cohesive areas) of trend types in the test area, confirmed the general patterns described above. This generalization procedure tended to eliminate areas with inconsistent trends, while evidencing areas with either full or partial consistency of trends (both negative and positive), providing a clearer picture of the spatial distribution of main temporal trends found in the analysed set of metrics. A predominant effect of the east-west climatic gradient is apparent, nonetheless the effects of local disturbances related to land use change, wildfires and others should not be neglected.

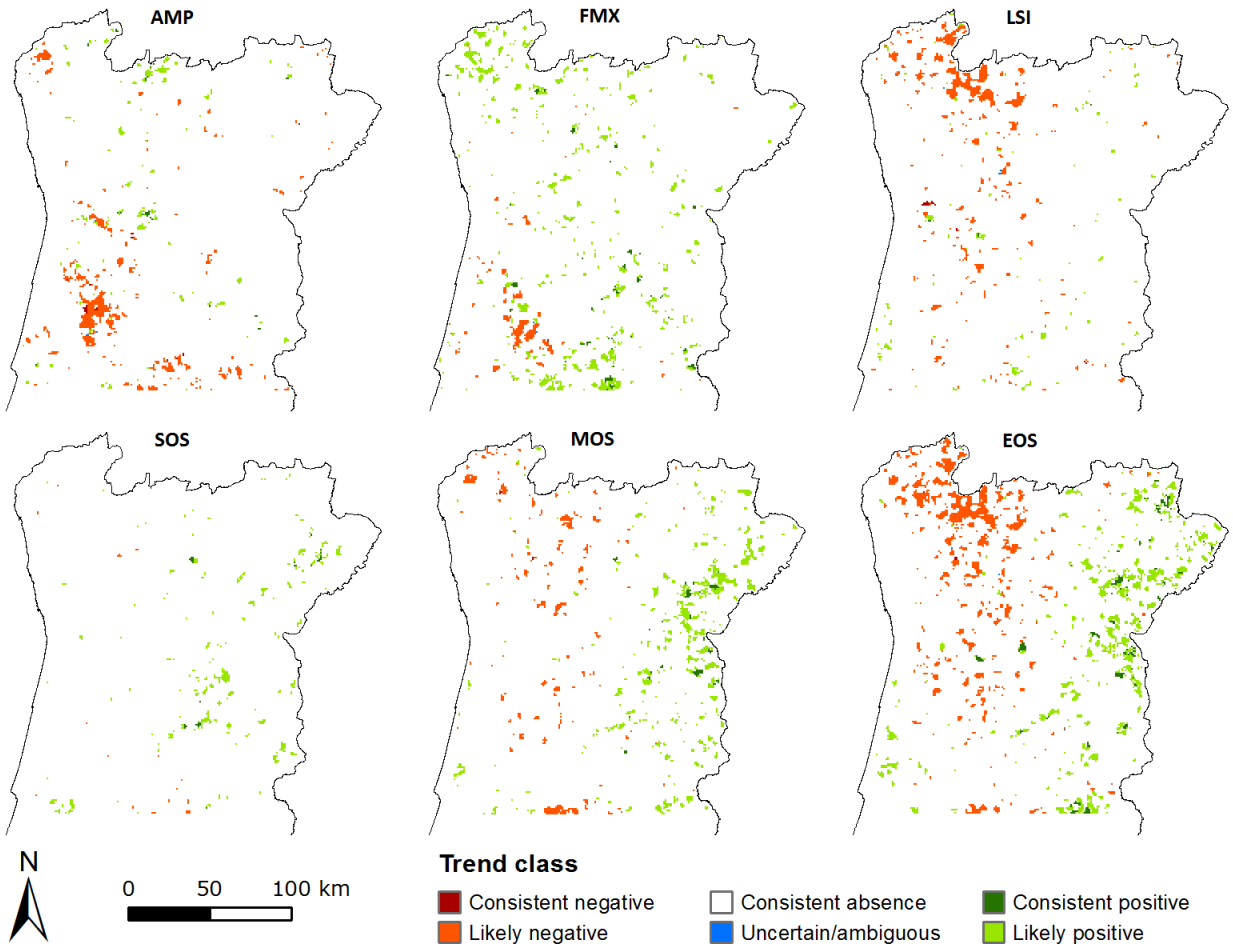

Figure 5: Identification of main spatial clusters of trend types of the selected TIMESAT metrics, in the test area, obtained by generalization of the corresponding consensus maps (see Figure 4) – "Seasonal amplitude" (AMP), "Largest data value for the fitted function during the season" (FMX), "Large seasonal integral" (LSI), "Time for the start of the season" (SOS), "Time for the mid of the season" (MOS), and "Time for the end of the season" (EOS). Classification of trends was based on the combinations of the types of trends ("Negative", "Positive" or "Absence") from each dataset used (MODIS and VGT).

The differences found in temporal trends of metrics derived from the NDVI annual curves may be explained by several factors. Red and near infrared bandwidths are slightly different between sensors, with both bands being wider for SPOT-5/VGT2 than for Terra/MODIS (Table 1). Radiometric resolution is also different between these two sensors – while MODIS is a 12-bit (i.e. 2^{12}grey levels per band) sensor, SPOT-VGT2 is an 8-bit sensor (i.e. 2^{8}grey levels per band). Therefore we have to consider that there may be differences in the sensitivity of each sensor to the phenomena studied here. Although we used datasets produced at the same spatial resolution (1km), the spatial resolution at which each sensor acquires the data used to produce these datasets is different (250m for MODIS and ~1km for SPOT-VEGETATION), which may have an influence on the NDVI values of the datasets like the ones used in this study. In turn, differences in the temporal resolution of the dataset used (composites of 16-day for MODIS, and 10-day for VGT) seem also to have had a considerable impact on results from the phenology metrics, and the corresponding trends, and for the metrics obtained from those (e.g. LSI). It should be noted however that, although the S10 VGT dataset has higher temporal resolution, it may also be more "noisy" (as observed in the analysis of signal-to-noise ratios for both sensors following the noise reduction procedures; data not shown), making the question "which dataset was/is more

accurate?" not easy to answer without some kind of field validation procedure or "ground truth" comparison available.

CONCLUSIONS

This work compares the temporal trends in key attributes of vegetation dynamics and ecosystem functioning derived from products obtained from two different satellite sensors – the MOD13A2 product from MODIS, and the S10 product from SPOT-VEGETATION (VGT2) – in the northern half of continental Portugal, in the 2003–2010 period. Consistency analysis revealed major differences in the use of these two datasets, in terms of direction and magnitude of the trends detected, as well as sensitivity to detect significant trends, especially for indicators of phenological attributes.

Different results from the analysis of trends in NDVI annual curves can lead to different conclusions about changes in attributes of vegetation dynamics and ecosystem functioning. Indicators derived from satellite data can be of great importance for regional scale environmental assessments, and they can provide important contributions to support decision-making and management policies, and especially for assessment and reporting purposes. With this in mind, our results suggest that the use of only one dataset for the assessment of trends in attributes of vegetation dynamics and ecosystem functioning should only be considered for cases where it would be possible to determine (e.g. using a validation strategy) which of the available datasets is more accurate for the area to be studied and the specific purpose(s). The use of phenological observation field stations may be a possible solution for validating outputs from temporal analysis of attributes of vegetation dynamics and ecosystem functioning obtained from satellite images. Nevertheless, those phenological observations are still not often available for a great variety of vegetation types or at the ecosystem level and their gathering is very time consuming. If no such information is available, approaches like the one used in this study, i.e. consistency analysis of outputs from two (or more) different sources (i.e. datasets/sensors), may be an alternative, allowing for at least an overall perspective of the main trends likely to have occurred in a target region and time window.

ACKNOWLEDGEMENTS

We thank Domingo Alcaraz (Departamento de Botánica, Faculdad de Ciencias, Universidad de Granada & CAESCG, Centro Andaluz para la Evaluación y Seguimento del Cambio Global, Universidad de Almería, Spain) for useful comments and remarks relating to early stages of the procedures and analyses supporting this paper.

REFERENCES

1 Kerr J T & M Ostrovsky, 2003. From space to species: ecological applications for remote sensing. Trends in Ecology and Evolution, 18(6): 299-305.

2 Glen E P, A R Huete, P L Nagler, S G Nelson, 2008. Relationship between remotely-sensed vegetation indices, canopy attributes and plant physiological processes: what vegetation indices can and cannot tell us about the landscape. Sensors, 8: 2136-2160.

3 Nagler P L, R L Scott, C Westenburg, J R Cleverly, E P Glenn & A R Huete, 2005. Evapotranspiration on western U.S. rivers estimated using the Enhanced Vegetation Index from MODIS and data from eddy covariance and Bowen ratio flux towers. Remote Sensing, 97: 337-351.

4 Pôças I, M Cunha & L S Pereira, 2012. Dynamics of mountain semi-natural grassland meadows inferred from SPOT-VEGETATION and field spectroradiometer data. International Journal of Remote Sensing, 33(14): 4334-4355.

5 Wilson T B & T P Meyers, 2007. Determining vegetation indices from solar and photosynthetically active radiation fluxes. Agricultural and Forest Meteorology, 144: 160-179.

6 Duro D C, N C Coops, M A Wulder & T Han, 2007. Development of a large area biodiversity monitoring system driven by remote sensing. Progress in Physical Geography, 31: 235-260.

7 Mildrexler D J, M Zhao & S W Running, 2009. Testing a MODIS Global Disturbance Index across North America. Remote Sensing of Environment, 113: 2103-2117.

8 Stoms D M & W W Hargrove, 2000. Potential NDVI as a baseline for monitoring ecosystem functioning. International Journal of Remote Sensing, 21: 401-407.

9 Bradley B A & E Fleishman, 2008. Can remote sensing of land cover improve species distribution modelling? Journal of Biogeography, 35: 1158-1159.

10 Jönsson, A. M., L. Eklundh, M. Hellström, L. Bärring, and P. Jönsson. 2010. Annual changes in MODIS vegetation indices of Swedish coniferous forests in relation to snow dynamics and tree phenology. Remote Sensing of Environment 114:2719-2730.

11 Strand H, R Höft, J Strittholt, L Miles, N Horning, E Fosnight & W Turner (eds.), 2007. Sourcebook on Remote Sensing and Biodiversity Indicators. Technical Series no. 32 (Secretariat of the Convention on Biological Diversity) 203 pp.

12 Alcaraz-Segura D, J Cabello, J M Paruelo & M Delibes, 2008. Trends in the surface vegetation dynamics of the National Parks of Spain as observed by satellite sensors. Applied Vegetation Science, 11: 431-440.

13 Anyamba A & C J Tucker, 2005. Analysis of Sahelian vegetation dynamics using NOAA-AVHRR NDVI data from 1981–2003. Journal of Arid Environments, 63: 596-614.

14 Fensholt R, K Rasmussen, T T Nielsen, C Mbow, 2009. Evaluation of earth observation based long term vegetation trends — Intercomparing NDVI time series trend analysis consistency of Sahel from AVHRR GIMMS, Terra MODIS and SPOT VGT data. Remote Sensing of Environment, 113: 1886-1898.

15 Zhao M & S W Running, 2010. Drought-Induced Reduction in Global Terrestrial Net Primary Production from 2000 Through 2009. Science, 329: 940-943.

16 Nemani R R, C D Keeling, H Hashimoto, W M Jolly, S C Piper, C J Tucker, R B Myneni & S W Running, 2003. Climate-Driven Increases in Global Terrestrial Net Primary Production from 1982 to 1999. Science, 300: 1560-1563.

17 Jobbágy E G, O E Sala & J M Paruelo, 2002. Patterns and controls of primary production in the Patagoninan steppe: A remote sensing approach. Ecology, 83: 307-319.

18 Jones M O, J S Kimball, L A Jones & K C McDonald, 2012. Satellite passive microwave detection of North America start of season. Remote Sensing of Environment, 123: 324-333.

19 Alcaraz-Segura D, J M Paruelo & J Cabello, 2006. Identification of current ecosystem functional types in the Iberian Peninsula. Global Ecology and Biogeography, 15: 200-212.

20 Alcaraz-Segura D, J Cabello, J M Paruelo & M Delibes, 2009. Use of descriptors of ecosystem functioning for monitoring a national park network: a remote sensing approach. Environmental Management, 43: 38-48.

21 Coops N C, M A Wulder, D C Duro, T Han & S Berry, 2008. The development of a Canadian dynamic habitat index using multi-temporal satellite estimates of canopy light absorbance. Ecological Indicators, 8: 754-766.

22 Paruelo J M & W K Lauenroth, 1998. Interannual variability of the NDVI curves and their climatic controls in North American shrublands and grasslands. Journal of Biogeography, 25: 721-733.

23 Paruelo J M, E G Jobbágy & O E Sala, 2001. Current distribution of ecosystem functional types in temperate South America. Ecosystems, 4: 683-698.

24 Milchunas D G & W K Lauenroth, 1995. Inertia in Plant Community Structure: State Changes After Cessation of Nutrient-Enrichment Stress. Ecological Applications, 5: 452-458.

25 Pettorelli N, J O Vik, A Mysterud, J-M Gaillard, C J Tucker, N C Stenseth, 2005. Using the satellite-derived NDVI to assess ecological responses to environmental change. Trends in Ecology and Evolution, 20: 503-510.

26 Piao S L, J Y Fang, W Ji, Q H Guo, J H Ke & S Tao, 2004. Variation in a satellite-based vegetation index in relation to climate in China. Journal of Vegetation Science, 15: 219-226.

27 Pouliot D, R Latifovic & I Olthof, 2008. Trends in vegetation NDVI from 1 km AVHRR data over Canada for the period 1985–2006. International Journal of Remote Sensing, 30: 149-168.

28 Tucker C J, D A Slayback, J E Pinzon, S O Los, R B Myneni, M G Taylor, 2001. Higher northern latitude normalized difference vegetation index and growing season trends from 1982 to 1999. International Journal Biometeorology, 45: 184-190.

29 Vicente-Serrano S M & A Heredia-Laclaustra, 2004. NAO influence on NDVI trends in the Iberian Peninsula (1982–2000). International Journal of Remote Sensing, 25: 2871-2879.

30 Alcaraz-Segura D, E Liras, S Tabik, J Paruelo & J Cabello, 2010. Evaluating the consistency of the 1982-1999 NDVI trends in the Iberian Peninsula across four time-series derived from the AVHRR sensor: LTDR, GIMMS, FASIR, and PAL-II. Sensors, 10(2): 1291-1314.

31 de Jong R, S de Bruin, A de Wit, M E Schaepman & D L Dent, 2011. Analysis of monotonic greening and browning trends from global NDVI time-series. Remote Sensing of Environment, 115: 692-702.

32 Verbyla D, 2008. The greening and browning of Alaska based on 1982–2003 satellite data. Global Ecology and Biogeography, 17: 547-555.

33 Xiao J & A Moody, 2005. Geographical distribution of global greening trends and their climatic correlates: 1982-1998. International Journal of Remote Sensing, 26: 2371-2390.

34 Metzger M J, R G H Bunce, R H G Jongman, C A Mücher & J W Watkins, 2005. A climatic stratification of the environment of Europe. Global Ecology and Biogeography, 14: 549-563.

35 Solano R, K Didan, A Jacobson & A Huete, 2010. MODIS vegetation indices (MOD13) C5 – User´s guide (The University of Arizona) 38 pp.

36 Holben B, 1986. Characteristics of maximum-value composite images from temporal AVHRR data. International Journal of Remote Sensing, 7(11): 1417–1434.

37 SPOT Vegetation User's Guide, 2011. Available online: http: //www.spot-vegetation.com/vegetationprogramme/Pages/TheVegetationSystem/userguide/userguide.html (last date accessed: 27 February 2012).

38 Bradley B A, R W Jacob, J F Hermance & J F Mustard, 2007. A curve fitting procedure to derive inter-annual phenologies from time series of noisy satellite NDVI data. Remote Sensing of Environment, 106: 137-145.

39 Hampel F, 1974. The influence curve and its role in robust estimation. Journal of the American Statistical Association, 69: 383–393.

40 Pearson R K, 2002. Outliers in process modeling and identification. IEEE Transactions on Control Systems Technology, 10(1): 55-63.

41 Savitzky A & M J E Golay, 1964. Smoothing and differentiation of data by simplified least squares procedures. Analytical Chemistry, 36(8): 1627-1639.

42 Chen J, P Jönsson, M Tamura, Z Gui, B Matsushita & L Eklundh, 2004. A simple method for reconstructing a high-quality NDVI time-series data set based on the Savitzky-Golay filter. Remote Sensing of Environment, 91(3-4): 332-344).

43 Heumman B W, J W Seaquist, L Eklundh & P Jönsson, 2007. AVHRR derived phenological change in the Sahel and Soudan, Africa, 1982-2005. Remote Sensing of Environment, 108: 385-392.

44 R Development Core Team, 2011. R: A language and environment for statistical computing, reference index version 2.14.1. R Foundation for Statistical Computing, Vienna, Austria. ISBN 3-900051-07-0, URL http://www.R-project.org.

45 Fensholt R & S R Proud, 2012. Evaluation of Earth Observation based global long term vegetation trends — Comparing GIMMS and MODIS global NDVI time series. Remote Sensing of Environment, 119: 131-147.

46 Jönsson P & L Eklundh, 2002. Seasonality extration by function fitting time-series of satellite sensor data. IEEE Transactions on Geoscience and remote sensing, 40: 1824-1832.

47 Jönsson P & L Eklundh, 2004. TIMESAT - a program for analysing time-series of satellite sensor data. Computers & Geosciences, 30. 833-845.

48 O'Connor B, E Dwyer, F Cawkwell & L Eklundh, 2012. Spatio-temporal patterns in vegetation start of season across the island of Ireland using the MERIS Global Vegetation Index. ISPRS Journal of Photogrammetry and Remote Sensing, 68: 79-94.

49 Fischer A, 1994. A model for the seasonal variations of vegetation indices in coarse resolution data and its inversion to extract crop parameters. Remote Sensing of Environment, 48: 220-230.

50 Hird J N & G J McDermid, 2009. Noise reduction of NDVI time series: An empirical comparison of selected techniques. Remote Sensing of Environment, 113 248-258.

51 Theil H, 1950. A rank-invariant method of linear and polynomial regression analysis, Part 3. Proceedings of Koninalijke Nederlandse Akademie van Weinenschatpen, 53: 1397-1412.

52 Sen P K, 1968. Estimates of the regression coefficient based on Kendall's tau. Journal of the American Statistical Association, 63: 1379-1389.

53 Bronaugh D & A Werner, 2009. zyp: Zhang + Yue-Pilon Trends Package. R Package Version 0.9-1.